J Nanopart Res
DOI 10.1007/s11051-007-9355-y

FOCUS ON NANOMANUFACTURING

Synthesis and post-processing of nanomaterials using microreaction technology

**Chih-Hung Chang · Brian K. Paul · Vincent T. Remcho ·
Sundar Atre · James E. Hutchison**

Received: 29 November 2007 / Accepted: 24 December 2007

Abstract A critical barrier to the routine use of nanomaterials is the tedious, expensive means of their synthesis. Microreaction technology takes advantage of the large surface area-to-volume ratios within microchannel structures to accelerate heat and mass transport. This accelerated transport allows for rapid changes in reaction temperatures and concentrations leading to more uniform heating and mixing which can have dramatic impacts on macromolecular yields and nanoparticle size distributions. Benefits of microreaction technology include higher yield and reactant conversion, better energy efficiency and less by-product generation. Microreactors can help minimize the environmental impact of nanoproduction by enabling solvent free mixing, integrated separation techniques and reagent recycling. The possibility of synthesizing nanomaterials in the required volumes at the point-of-use eliminates the need to store and transport potentially hazardous materials and provides the flexibility for tailoring complex functional nanomaterials. Recognizing these benefits for nanosynthesis, continuous flow microreactors have been used by several research groups to synthesize and characterize nanomaterials. An overview of these efforts and issues related to scale up and other post synthesis processes such as separation and deposition are presented in this paper.

Keywords Microreactors · Microreaction technology · Scale up · Nanoparticles · Dendrimers · Production · Separation · Deposition · Nanomanufacturing

Introduction

Microscale process engineering is the science of conducting chemical or physical processes (unit operations) inside small volumes, typically inside channels with diameters of less than 1 mm (microchannels) or other structures with sub-millimeter dimensions. These processes are usually carried out as continuous production, compared to batch production, with the potential to make microscale process

---

C.-H. Chang (✉)
School of Chemical, Biological and Environmental Engineering, Oregon State University, Corvallis, OR 97331, USA
e-mail: changch@engr.orst.edu

B. K. Paul · S. Atre
School of Mechanical, Industrial and Manufacturing Engineering, Oregon State University, Corvallis, OR 97331, USA

V. T. Remcho (✉)
Department of Chemistry, Oregon State University, Corvallis, OR 97331, USA
e-mail: vincent.remcho@oregonstate.edu

J. E. Hutchison
Department of Chemistry, Materials Science Institute, University of Oregon, Eugene, OR 97403, USA

engineering a tool for chemical production. Microscale process engineering involves the integration of various microscale unit operations being developed within many commercial applications including micromixers and microreactors for the pharmaceutical and fine chemical industry, lab-on-a-chip devices, microsensors, rapid throughput chemical and catalyst screening tools, distributed or portable power and chemical production, distributed heating and cooling, and even space applications (Hessel et al. 2004). Novel fabrication and processing techniques, equipment, and operational methods are resulting in developments that go beyond traditional chemical engineering. These new developments promise the transformation of process plants into compact, safe, energy-efficient, and environmentally sustainable processes (Fig. 1).

A microreactor is a device that enables chemical reactions to be done on the micrometer scale. They are miniaturized chemical reaction systems, which contain reaction channels with a typical diameter of 10–500 microns. The small channel dimensions lead to a relatively large surface area-to-volume ratios and increased driving forces for heat and mass transport (Hessel et al. 2004). Microreactors are especially suited for fast reactions with a large heat effect, where they allow for nearly isothermal conditions at high reactant concentrations, which is not possible in macroscale reactors. The possibility of fast mixing of reactants and fast heating and cooling of reaction mixtures enables precise control of the reaction parameters, thus improving the yield of reaction intermediates while reducing by-product formation.

Synthesis of nanomaterials using microreactors

An important application of microreactors is for the synthesis of nanomaterials. (deMello 2006; deMello and deMello 2004). For example, nanoscale ceramic powders can help significantly in the miniaturization of current products and can be used for various high performance applications due to their excellent mechanical, thermal, dielectric and corrosion properties (Ritter 2002). The performance of these nanoscale ceramic powders is strongly affected by particle properties, such as the particle size, the distributions of the size, and the shape. Conventionally large-scale batch reactors have been used for the synthesis of ceramic nanoparticles. However, the size distribution of nanoparticles synthesized in large scale batch reactors often does not satisfy the requirements for many applications. This is because the rate of forming fine particles is much faster than

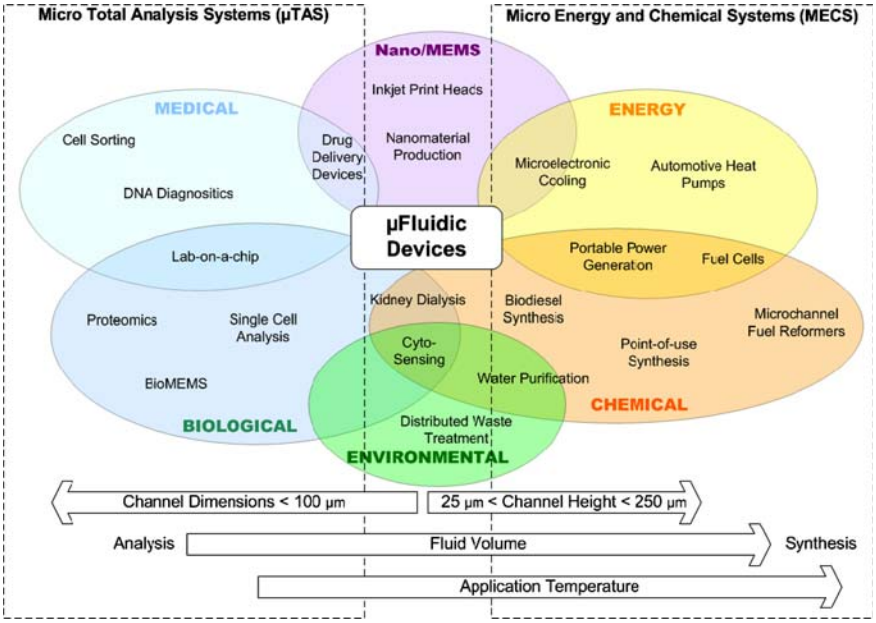

Fig. 1 Schematic representation of various microfluidic devices in different applications

the mixing rate of the reactant. To overcome this problem, microreaction technology has been attracting attention as a method for nanoparticle production. A microreactor provides control over the mean residence time, mixing and reaction temperature and hence over the nanoparticle size and shape. Decrease of linear dimensions increase the gradient of temperature, concentration, and chemical potential that are critical for processing. The driving force for heat transfer and mass transfer increase dramatically.

Typical fluid layer thickness in micromixers can be scaled down to a few tens of micrometers. Consequently, in micromixers, mixing times of milliseconds can be easily achieved. Several groups have taken advantage of micromixing to achieve fast, controllable and uniform mixing to synthesize nanoparticles. Edel et al. (2002) used a micromixer for the controlled production of CdS nanoparticles in aqueous solution (see Fig. 2). A microfabricated mixer based on the principle of distributive mixing and flow lamination was used to achieve fast mixing of $CdNO_3$ and Na_2S in aqueous solution in the presence of a sodium polyphosphate stabilizer. It was found that the use of the microreactor lowered the polydispersity of CdS nanoparticles.

Wagner and Köhler (2005) used a chip-based micromixer fabricated from silicon and glass to synthesize Au nanoparticles in the size range from 5 to 50 nm. The mixing is based on split and recombined lamellae of the laminar streams of the solution and the mixer contains eight split and recombination zones. A narrower size distribution was obtained from the microreactor than from the conventional approach.

Microreactors have found applications for controlled synthesis of polymer particles (Bouquey et al. 2007) and dendrimers (Liu et al. 2006, 2008). Dendrimers are nanoscale macromolecules that have highly branched, core-shell structures. Higher generation dendrimers have close-packed peripheral functional groups and a hollow interior. The chemistry of the core and the terminal functionalities can be tailored according to the specific application. These unique features have led dendrimers to a large number of potential applications. Dendrimers are synthesized in a stepwise manner to higher generations using a number of chemical reactions, so carrying out the synthesis in a conventional reactor is time-consuming. Therefore the dendrimer products are expensive. Liu et al. (2006, 2008) have synthesized dendrimers through both divergent and convergent routes by using a continuous flow microreactor. The microreactor consisted of an interdigital micromixer for enhanced mixing and microchannels for fast heat transfer. Using the microreactor, dendrons and dendrimers were synthesized within seconds of residence time. In comparison, the conventional flask synthesis took several hours or days for a similar yield.

Microreactors offer large interfacial areas per unit volume (10,000–50,000 m^2/m^3) which is much higher than the surface area-to-volume ratio of conventional reactors (100 m^2/m^3). For example, an integrated microchannel heat exchanger could provide heat transfer coefficients up to 26,000 W/m^2 K which is an order of magnitude higher than conventional heat exchangers (Kochmann 2006). This feature facilitates fast and accurate temperature control for nanoparticle synthesis. In general, it takes only seconds or sub-seconds to raise a solution in a microchannel from room temperature to hundreds of degree C. CdSe nanocrystals, also called quantum dots, have found applications including biological fluorescent labels, tunable LEDs, and solar cells.

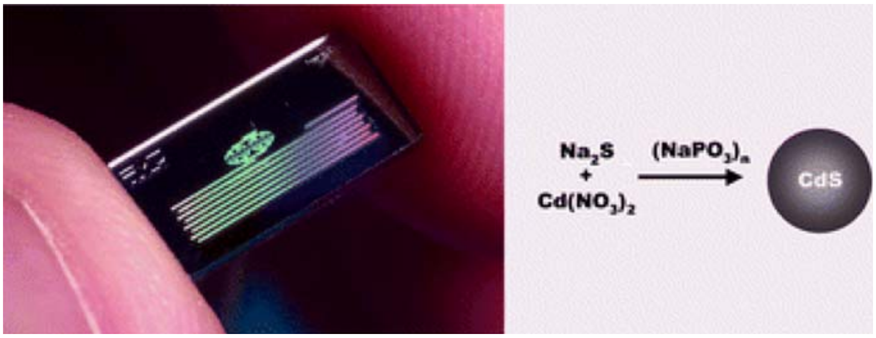

Fig. 2 The chip-based microreactor for the synthesis of CdS nanoparticles (image reproduced from Edel et al. 2002 with permission)

High quality CdSe nanocrystals were synthesized by rapid injection of organometallic precursors into a hot coordinating solvent. However, the quality and size control in the batch process depends strongly on factors that are difficult to control and scale up. Thus, several research groups have investigated the use of microreactors for the synthesis of CdSe. Nakamura et al. (2002) is the first to demonstrate this advantage through the synthesis of CdSe semiconductor nanocrystals using a microcapillary reactor (see Fig. 3). CdSe nanocrystals of different sizes were synthesized continuously and reproducibly by simply varying the temperature.

Chan et al. (2003) demonstrated the use of microfabricated chip-based reactors for the high-temperature synthesis, control and characterization of high quality CdSe nanocrystals. The microreactor included a heating zone for temperature control and mixing elements for pre- and post-reaction dilution. The fluorescence spectra of CdSe nanocrystals were monitored continuously at the end of the reactor using an external capillary flow cell. Yen et al. (2003) synthesized CdSe nanocrystals using a continuous-flow microreactor. This microreactor consisted of a miniature convective micromixer, a glass capillary tube, and a cartridge heater. A series of experiments were performed on important process parameters including temperature, residence time, and Se:Cd precursor ratio. Krishnadsan et al. (2004) focused their studies on the influence of residence time distribution and temperature in a chip-based microreactor. Lin et al. (2004) synthesized silver nanoparticles in a continuous flow tubular microreactor using silver pentafluoropropionate as a single-phase reactant precursor. Uniform size silver nanoparticles were obtained through thermal reduction of silver pentafluoropropionate in isoamyl ether within minutes.

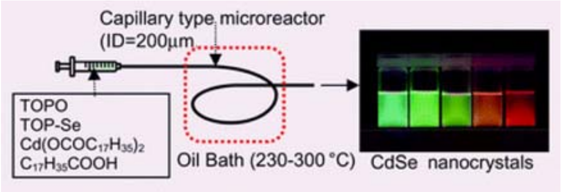

Fig. 3 Synthesis of CdSe nanocrystals using a capillary microreactor (image reproduced from Nakamura et al. 2002 with permission)

Microreactors provide opportunities to obtain uniform and well-defined fluid flows that could benefit nanosynthesis. Sounart et al. (2007) examined the synthesis of cysteine-capped CdS nanocrystals between two interdiffusing reagent streams. The laminar flow allowed for controlled diffusional mixing of the reacting cadmium and sulfide ions at the boundary between the two solutions, while the capping agent was present in one or both, the solution was in excess. The spatially resolved nucleation and growth in the reactor was exploited using an epifluoresence microscope. Kroon et al. (2003) studied the effects of different mixing styles on the coagulation processes by synthesizing CdS nanoparticles without the use of stabilizers. The studies show that the use of the micromixer and laminar flow reactor demonstrates enhanced colloidal stability. This can be attributed to the lack of turbulence and fluid motion, which increases the rate of particle aggregation. Perikinetic aggregation occurs as a result of collisions due to Brownian motion (Elimelech et al. 1998). Such collisions are dependent upon the ability of the particles to move within the solution medium, generally quantified by the diffusion coefficient of the substance. These quantities are influenced by the fluid medium, the temperature and the size of the particles themselves, with the value decreasing with increasing particle size. Orthokinetic aggregation is the result of particles colliding due to transport by the fluid motion (Elimelech et al. 1998). Both of these effects contribute to aggregation in batch reactor systems. In order to eliminate the orthokinetic effects it would be necessary to inhibit the stirring mechanism. Without stirring the solution, however, the diffusion distance would be quite large and the chance of having anything close to burst nucleation would be significantly decreased. It should also be noted that as particle size increases the orthokinetic aggregation has a stronger and stronger effect. Within microreactors, all fluid flow is laminar and well ordered. There is little chance of particles being forced to collide as a result of the fluid pushing them together as there are no shear forces between fluid elements. Therefore the movement of individual particles, like the movement of the ions in nucleation, is dependent upon diffusion and random Brownian motion. Thus, the presence of orthokinetic aggregation is eliminated.

The nanocrystal size distribution depends on the residence time distribution caused by axial dispersion effects due to the parabolic flow profile. Segmented flow microreactors offer an opportunity to solve the dispersion issue. Both gas–liquid and liquid–liquid microreactors have been reported. Kahn et al. (2004) examined the synthesis of SiO_2 nanoparticle using laminar flow and segmented flow reactors. Microreactors were fabricated in poly(dimethylsiloxane) (PDMS) by using soft lithography technique. The reactors included micromixers, gas injection nozzles, and aging channels. Laminar flow reactors produced wider particle size distribution at higher linear velocity caused by axial dispersion. Gas was used to generate segmented flow with liquid plugs separated by inert gas bubbles. The internal recirculation in the liquid plugs enhances mixing and reduces the axial dispersion effects and produces a narrower size distribution. Alternatively, droplet-based microreactors have also generated segmented flow from two immiscible liquids. Shestopalov et al. (2004) synthesized CdS and CdS/CdSe nanoparticles using aqueous droplets in fluorocarbon oil. Winding channels help rapidly mix the reagents in droplets. Direct injection of aqueous reagent into flowing droplets was performed to achieve multi-step, time controlled syntheses of CdS/CdSe core-shell nanoparticles (Fig. 4). Chan et al. (2005) synthesize CdSe nanocrystals in nanoliter droplets flowing in a perfluorinated carrier fluid through a microfabricated reactor. The reactor included a flow-focusing nanojet structure with a step increase in channel height. The encapsulation of the reaction within liquid droplets physically isolated reactants from channel walls so no deposition on the wall would occur.

These high interfacial areas not only provide large heat transfer surfaces but also allow unique opportunities for running multiphase processes. Wang et al. (2002) synthesized TiO_2 nanoparticles by using a stable interface between two insoluble currents in a microchannel reactor. Two insoluble liquid systems 1-hexanol/formamide and cyclohexane/water were used. The hydrolysis reaction between titanium tetraisoproxide (TTIP) and water occur at the interface to form titania. Mae et al. (Takagi et al. 2004; Nagasawa et al. 2007) performed similar reaction to synthesize titania nanoparticles by an annular laminar flow of two immiscible liquids. The microreactor consists of an external glass pipe of inner diameter 1,500 μm and an internal stainless pipe of outer diameter 460 μm and inner diameter 320 μm. The pipes are placed coaxially, forming a dual pipe structure. Annular flow, slug flow, and dispersive flow were obtained depending on the flow rates of inner and outer fluids and the properties of the fluids. It was found that a stable annular flow is formed under a large ratio of inertial force to the interfacial tension and small difference in the velocities between the inner and outer fluids. Titania nanoparticles with controllable size in the range from 3 to 150 nm were produced by changing the diameter of the inner tube at a low TTIP concentration.

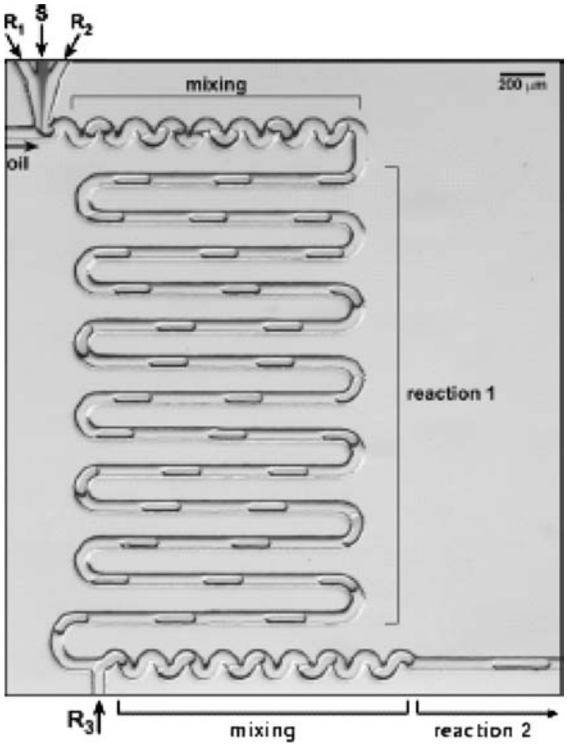

Fig. 4 A microfluidic device for performing droplet-based two step synthesis (image reproduced from Shestopalov et al. 2004 with permission)

Scale-up of microreactors

Many researchers have demonstrated the advantages of microchannel processing of nanomaterials over conventional batch processing including lower production cost, safer operation, improved selectivity, reduced energy consumption and better process control. While claims have been made for ease of scale-up, the technical literature does not provide any scale-up demonstrations for the microchannel processing of nanomaterials. In order for the microchannel processing of nanomaterials to be industrially viable, scale-up of parallel microchannels must be established with each microchannel processing equivalent amounts of fluid under precise concentrations and temperatures and small residence time distributions. While microreactor scale-up has been demonstrated for certain polymerization reactions (Schenk et al. 2004) and has been discussed for general chemistry (Taylor et al. 2005; Fournier et al. 1996; Schenk et al. 2003), the discussion below will serve to focus scale-up issues associated with the microchannel processing of nanomaterials.

Scale-up fundamentally involves increasing the volumetric flow rate through the microreaction system according to the equation:

$$\dot{v} = V_{\mathrm{avg}} \cdot A \tag{1}$$

where $\dot{v}$ is the volumetric flow rate of reactants through microchannels, V_{avg} is the average velocity of the reactants through the microchannels and A is the flow cross-section which is a product of the flow cross-section of each microchannel by the number of microchannels. Increasing the average velocity through the microchannels increases the pressure drop across the microchannel which is practically limited by the size of the pump. A more reasonable strategy involves increasing the cross-section of flow by arraying parallel microchannels. In the general microreactor literature, this scale-up strategy is called "numbering up" (Ehrfeld et al. 2000). In this article, we define scale-up to be the processing of an industrially relevant flow rate sustained by a large array of parallel microchannels (hundreds to millions).

As shown in Table 1 below, at least three levels of numbering-up can be considered for increasing the flow cross-section of microchannel architectures.

"Channel up" is the most fundamental level of scale-up and typically involves arraying identical channels within a confined material layer or lamina. Ultimately, this strategy is constrained by the size of the microchannel and the size of the lamina used. Manufacturing processes are typically limited in the size of the laminae that can be processed and so impose the ultimate constraint on channel-up strategies. Additional channels can be added using a "layer up" strategy where additional laminae are added each containing identical "channel up" arrays. The constraint on this strategy is typically the thickness of the laminae and the work envelope of the bonding process used to convert the laminae into a monolith. As shown in Fig. 5, microlamination (Paul and Peterson 1999) architectures, involving the patterning and bonding of thin laminae, employ these two strategies for scaling-up microchannel arrays (Paul 2005). Beyond this, a "device up" strategy is used to increase throughput by simply adding identical devices in parallel.

Contrary to the popular technical literature, these scale-up strategies are not free from difficulties. The most undesirable effect of a parallel microchannel reaction architecture is variation in reaction conditions. Variations in concentration, temperature and residence time can all be detrimental to nanoparticle size distributions. The most difficult of these to control is residence time. Poor residence time distributions can be due to both flow velocity profiles within microchannels as well as flow maldistribution between microchannels.

For the large class of homogeneous liquid-phase reactions, microreactors are frequently based on single-phase laminar flow designs. However, as indicated above, such designs are restricted in terms of wide residence time distributions (RTDs). Yen et al. (2005) showed progress toward improving RTDs by using recirculation within two-phase segmented flows (gas–liquid or liquid–liquid) to eliminate axial dispersion as encountered in single phase laminar flow. Jongen et al. (2003) precipitated out $CaCO_3$ using a segmented flow microreactor and established that the particle size distribution is narrower than the commercially available powders.

Table 1 Three different levels for numbering up microreactors

Device up	Layer up	Channel up
Identical devices are connected in parallel through interconnects	Identical layers or laminae are stacked and bonded together	Identical channels are arrayed on a single lamina

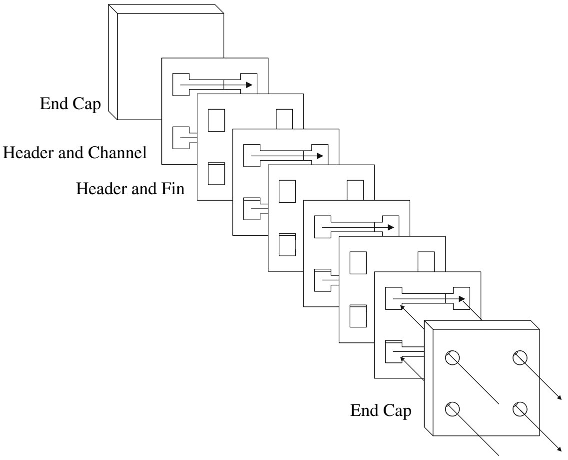

Fig. 5 Microlamination architecture used to fabricate a dual micro-channel array. Channel-up and layer-up strategies are both illustrated. *Arrows* show direction of flow

The dispersion span ($d_{v90} - d_{v10}/d_{v50}$) was reduced from 1.69 to 1.09. Experiments were also conducted with $BaTiO_3$ and it was found that the produced powder had much smaller particle size (30 nm) with high specific surface area (40 m^2/g) compared to commercially available high purity fine powder having particle size (60 nm) with specific surface area of 17 m^2/g. Recirculation has the dual effect of narrowing the RTD as well as improving mixing. In contrast to single-phase designs, segmentation makes it possible to drive reactions to required yields over significantly shorter times owing to the enhanced mixing, while maintaining narrow RTDs and producing narrowly dispersed powder particles (Ismagilov 2003). The schematic representation of laminar flow and segmented flow is shown in Fig. 6.

However, this condition is strictly true only if neighboring slugs of the phase of interest are completely disconnected from each other. Therefore, in designing microchannel reactors, it is important to minimize sharp changes in flow direction. Using a segmented gas-liquid flow system, Trachsel et al. (2005) found, in maneuvering around sharp radii, adjacent liquid slugs were connected across thin liquid films or menisci. Khan et al. (2004) compared a single phase laminar flow reactor (LFR) with a segmented flow reactor (SFR) in producing silica nanoparticles. The results showed that the latter had smaller particle size distribution compared to the continuous single phase microreactor (LFR: residence time: 6.5 min, average particle size: 281 nm with a standard deviation of 20%; SFR: residence time: 10 min, average particle size: 277 nm with a standard deviation of 9.5%). The thickness of the film depended on the relative magnitude of viscous to surface tension forces using the dimensionless capillary number, C_a:

$$C_a = \frac{\mu U_b}{\sigma} \tag{2}$$

where μ is the liquid viscosity, U_b is bubble velocity and σ is the interfacial tension. Based on Betterton's model, it was predicted that rectangular channels would have ~2–3 times increase in the communication between neighboring liquid slugs than circular channels with the same cross-sectional area (Yen et al. 2003). Several research groups have reported other techniques to introduce segmented (slug) flow inside a microchannel system, typically based on the application of external pneumatic, magnetic, ultrasonic, or electrical energy (Glasgow and Aubry 2003).

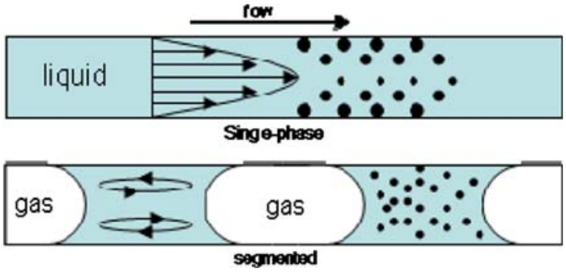

Fig. 6 Single phase laminar flow versus segmented flow (Yen et al. 2003)

In recent years, there has been considerable focus on equalizing the flow distribution across microchannel arrays. Most of this work has been undertaken outside the field of nanomaterial synthesis. In addition to effecting residence time distributions, fluid velocities across microchannels affect the heat and mass transfer throughout the device (Wiessmeier et al. 1998). To equilibrate flow velocities, an appropriate "channel-up" structure is required to distribute the flow from a common reactant reservoir through the microchannels to a common product reservoir. Amador et al. (2004) studied two different kinds of manifold structures, namely consecutive and bifurcated, using a method based on electrical resistance circuit analysis and validated against finite element simulations. An analytical model was also developed to study the effects of manufacturing tolerances and of channel blockage on flow distribution. The bifurcation manifold structure was found to be better for uniform flow distribution. Commenge et al. (2002) evaluated flow distribution in a multichannel microreactor having a consecutive type of manifold structure to distribute the reactant fluid to the microchannels. An optimum reactor design was found for a single-phase flow distribution that gave almost a uniform flow distribution. The analysis was performed using a resistance network method combined with an optimizing function to calculate varying diameters for flow distribution and collection channels. Bejan and Errera (1997) compared fractal tree-like structures to naturally available structures like lungs, arteries, veins etc. and found that these structures not only give flow uniformity but also minimized flow resistance through a volume-to-point path. Ajmera et al. (2002) developed a novel design of a silicon cross-flow microreactor for parallel testing of porous catalyst beds. The uniform flow distribution was achieved by bifurcating the inlet stream into 64 parallel microchannels. The experimental data was validated using computational fluid dynamics (CFD) models.

Uniformity of the flow distribution must also involve equalizing and distributing flow between layers and devices. At a device level, the non-uniformity of fluid flow in a microchannel reactor system is primarily attributed to the difficulty in making a smooth transition from the cross sectional shape of a reactor to that of the upstream and downstream connectors without any dead volume (Rebrov et al. 2003). At a layer level, the methods for uniformly distributing fluid within multilayered structures vary based on differences in the geometry of the inlets and the outlets of the reactor units. Baffles can be used to create backpressures upstream of the array. Screens have been found to be a simple and effective means to uniformly distribute flow throughout the cross-section of macro-scale reactors. Several researchers have evaluated the use of different kinds of meshes and screens for solving the problem of flow equalization between microchannel layers (Idelchik 1994). The screen leveling properties depend on the geometrical parameters like effective (open) cross-section and the thickness of the screen. The drag co-efficient, ζ, of the screen can be defined as

$$\zeta = \frac{2\Delta p}{\rho \cdot V_{\mathrm{avg}}^2} \tag{3}$$

where Δp is pressure drop along the screen, ρ is the density of the fluid and V_{avg} is the average velocity. A flow distribution system is desired if ζ of the screen is less than 1,000 (Idelchik 1991). Riman and Cherepkova (1973) proposed a method for calculating the distortion in velocity profile using a similar grid concept. Most of these methods have been developed for macro-scale reactors under turbulent flow regimes having high Reynolds number, which is not the case in microreactor systems. However, Rebrov et al. (2007) (Mies et al. 2006) proposed a conical diffuser connected to a thick-walled screen to enhance the uniformity of fluid flow distribution within micro-scale reactors. The design of the header was optimized using CFD simulations. Numerical simulations suggested that the proposed header configuration including screens can effectively improve the performance of the microreactor, decreasing the ratio of the maximum velocity to the mean flow velocity to between 1 and 2 for a wide range of Reynolds numbers (0.5–10).

The head loss associated with flow through an interconnect–header interface is a common minor loss. The purpose of a header is to regulate the flow distribution between layers and channels in the system. The most common method for determining these head losses or pressure drop is to specify a loss factor, K_{L}

$$K_{\mathrm{L}} = \frac{h_{\mathrm{L}}}{\left(V_{\mathrm{avg}}^2/2g\right)} = \frac{2\Delta p}{\rho \cdot V_{\mathrm{avg}}^2} \tag{4}$$

where h_{L} is the head loss between sections having areas A_1 (inlet) and A_2 (outlet), V_{avg} is the average velocity of the fluid, Δp is the pressure drop and ρ is the density of the fluid. K_{L} is a function of geometry of the component and Reynolds number, R_{e}. A fluid may flow from a headers into a channel through any number of different shaped entrance regions, namely square, round, conical (downstream) or vise versa (upstream) (Fig. 7). As a fluid enters into a square-edged entrance (Fig. 7a), there is vena contracta (which results in a dead volume because of contraction) developed because the fluid cannot make a sharp right-angled corner. At the vena contracta region, the kinetic energy of the fluid is partially lost because of

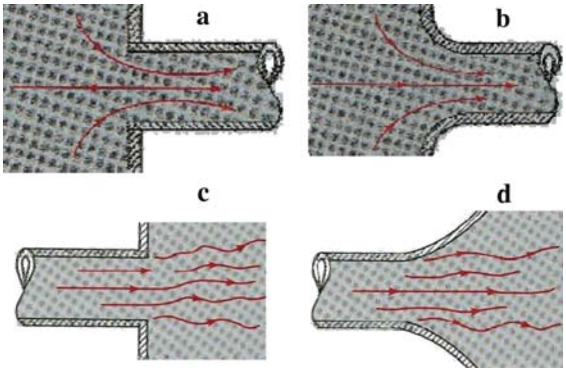

Fig. 7 Entrance flow (upstream) conditions (**a**) $K_L = 0.5$ (**b**) $K_L = 0.04$ and exit flow (downstream) conditions (**c**) $K_L = 1$ (**d**) $K_L = 1$

viscous dissipation and an entrance or exit head loss is generated (Munson et al. 1994). For a micromixer, this vena contracta on the reaction (Fig. 7a) side can significantly affect the residence time distribution. It is anticipated that conical diffusers, with varying area ratios, A_1/A_2, can be used to better regulate the flow distribution. Figure 8 shows the effect of the included angle of the diffuser, θ, on the velocity head through an expansion which is the typical situation for a microreactor outlet. Sovran and Klomp (1967) reported that the optimum angle for minimum loss co-efficient under these conditions is $\theta = 8°$.

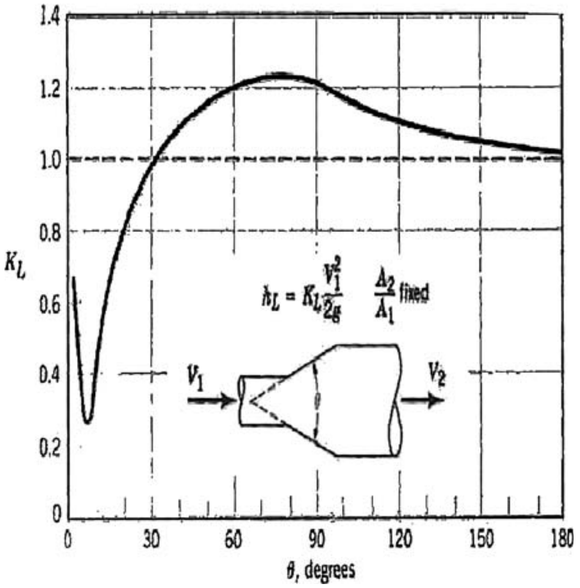

Fig. 8 Loss co-efficient K_L for a typical conical diffuser (image reproduced from Sovran and Klomp 1967)

Post synthesis processing

Size-based separations: ensuring nanomaterial product integrity

Separation of nanoparticles by size is of particular importance since their properties and applications are size-dependent. A number of filtration, chromatographic and electrophoretic methods have been applied for purification and separation of nanomaterials from byproducts and into different sizes. Here we review the various approaches taken to date in this young but growing field of study.

Continuous-mode separations: filtration methods for microfluidic purification of nanoparticles

The terminology and definitions of filtration vary somewhat from source to source. However, some generalities can be drawn. Filtration, in the broadest sense, is discrimination of a fluid mixture through a phase barrier and across a gradient. A familiar example is an aqueous suspension drawn through filter paper by gravity. However, fluids include both the liquid and gas phase. Phase barriers come in a variety of forms and are generally referred to as membranes. Gradients are usually, but not limited to, pressure and concentration. Through all of this, three terms remain well defined: the mixture to be filtered is the feed, that portion which passes through the membrane is the permeate, that which does not is the retentate.

An attempt can be made to characterize membranes as either porous or nonporous. A porous membrane has passages from one side to the other through which solvent, solutes and small particles can be transported via convection or diffusion to the other side to become part of the permeate. Size discrimination is an obvious consequence of either fitting through the hole or not. A nonporous membrane is lacking such passages. Solvent and solute must dissolve into the membrane, diffuse across the membrane thickness and redissolve out the other side in order to become part of the permeate. Since smaller solute molecules diffuse faster than larger solute molecules, size discrimination tends to be preserved. Keep in mind, on the nanoscale care must be taken when attempting to distinguish between molecule and nanoparticle, solute and suspended particle, pore space and interstitial space between polymer chains.

A separate membrane characterization is based on electrostatic charge. A membrane with a surface charge will tend to reject species with similar charge but pass oppositely charged and neutral species. This effect is, of course, highly dependent upon pH of the solution and isoelectric points of solute species and the membrane itself. Since charge interactions are inversely proportional to the square of the distance, the surface of a small diameter pore will have a much greater influence on charged species transport that that of a larger diameter pore.

The performance of a filtration membrane with respect to a specific species is usually expressed in terms of rejection (5) and is often stated as percent rejection. A rejection of 100% indicates that the membrane retained all of a particular species. Whereas a rejection of 0% indicates that the membrane retained none of that species. Rejection is dependent upon many factors including concentration, pressure and flow conditions.

$$\text{Rejection} = 1 - \frac{\text{Permeate Concentration}}{\text{Retentate Concentration}} \tag{5}$$

Filtration membranes are typically rated by a molecular weight cutoff (MWCO), defined as the molecular weight of a species with 90% rejection. This means that the relative concentrations of that particular species in the retentate and permeate will be 10:1 as a result of the filtration. This value is meant to serve only as a rough estimate for predicting membrane performance with other species since it does not take into account possible variables such as molecular shape, charge effects or interactions such as adhesion, partitioning or swelling.

A combination of flow configurations can be realized depending upon the application needs or design restrictions. Dead end flow, in which the feed flows orthogonal to the membrane surface, tends to be limited by issues such as concentration polarization and fouling of the membrane. Cross flow, in which the feed flows tangential to the membrane surface, is employed to minimize such effects. A sweep of solvent can be used to enhance transport in the permeate. Co-current refers to a sweep flowing in the same direction as the feed, whereas counter current is in the opposite direction. Diafiltration refers to a method in which the retentate is recirculated along with additional solvent into the feed in order to maintain a constant volume (Fig. 9).

Demands for structural strength, chemical compatibility and surface charge have driven the development of a wide variety of polymeric and inorganic materials far too numerous to detail here. Membrane architectures tend to fall neatly into two categories: symmetric (isotropic) and asymmetric (anisotropic). Symmetric membranes have a uniform structure with no orientation such as the simple fibrous filter paper example given above. Asymmetric membranes consist of a thin, selective active layer bound to a thicker layer for mechanical support.

There are several categories into which the spectrum of filtration has been divided: microfiltration, ultrafiltration, nanofiltration and reverse osmosis (6). Each is based loosely on a MWCO range expressed in Daltons (Da).

$$\begin{aligned}&\text{microfiltration} > 1000\text{ kDa} > \text{ultrafiltration} >\\&1\text{ kDa} > \text{nanofiltration} > 0.1\text{ kDa} > \text{reverse osmosis}\end{aligned} \tag{6}$$

Recent work has demonstrated that filtration techniques can successfully be applied to purification and size fractionation of nanoparticles. As with many synthetic processes, excess materials such as precursors, salts, monomers and emulsifiers must be removed in order to purify the desired product. Fortunately, most of these materials are smaller in mass than the synthesized nanoparticle. Ultrafiltration methods have been used for post-synthetic purification of aluminum, gold and polymer nanoparticles in aqueous environments (Gautam et al. 2005; Huang

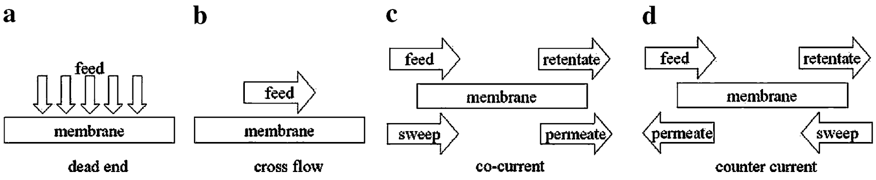

Fig. 9 Schematics of flow configurations commonly used in filtration processes

et al. 2006; Sweeney et al. 2006; Tishchenko et al. 2001). Nanofiltration methods have been used for post-synthetic purification of gold and polymer nanoparticles in organic solvent environments (Akthakul et al. 2005; Rundel et al. 2007). Size fractionation of polydisperse gold nanoparticles has been demonstrated using both ultrafiltration and nanofiltration methods (Sweeney et al. 2006; Rundel et al. 2007).

Batch-mode separations: separation and purification of nanomaterials using chromatographic and electrophoretic methods

To date, several chromatographic and electrophoretic methods have been employed for the separation of nanomaterials. Gel permeation chromatography (GPC) (Zhao et al. 2001; Niyogi et al. 2001; Al-Somali et al. 2004; Chattopadhyay et al. 2002; Krueger et al. 2005; Wei and Liu 1999; Wei et al. 1999; Siebrands et al. 1993), Capillary electrophoresis (CE) (Schnabel et al. 1997; Xu et al. 2004), Reverse-phase high-performance liquid chromatography (RP-HPLC) (Wilcoxon et al. 2000; Jimenez et al. 2003) and Ion exchange chromatography (IEX) (Jahanshahi et al. 2005; Bas et al. 1998) have all met with various levels of success. GPC offers an ideal solution for both nanoparticle characterization and batch-mode, small-process scale separation according to size.

Larger diameter nanoparticles are excluded from the pores of the chromatographic column, and therefore elute in decreasing order of their hydrodynamic volume (largest first) provided that no interaction occurs between the nanoparticles and the surface of the packing material. GPC has proved a powerful size-based purification and separation method for carbon nanotubes (Zhao et al. 2001; Chattopadhyay et al. 2002), nanocrystalline CdSe (Krueger et al. 2005) and gold nanoparticles (Al-Somali et al. 2004; Wei and Liu 1999; Wei et al. 1999; Siebrands et al. 1993) To minimize adsorption on the column packing material a series of additives had to be used in the mobile phase, such as surfactants (Wei and Liu 1999; Wei et al. 1999), citrate and tannin (Siebrands et al. 1993), or chemical modifications of the nanomaterial surface had to be made (Niyogi et al. 2001; Al-Somali et al. 2004; Krueger et al. 2005; Siebrands et al. 1993). Variation of the composition of surfactant mixture in the mobile phase allowed a GPC separation based on differences in *shape* for rodlike and spherical gold nanoparticles (Wei et al. 1999).

Wilcoxon et al. (2000) used solid-phase extraction cartridges filled with HPLC packing material to purify alkane thiol-stabilized Au nanoclusters. They took advantage of the lack of interaction between neutral gold nanoparticles and the stationary phase which passed freely through the column while ions and surfactants were retained. Jimenez et al. (2003) separated alkanethiolate-coated gold clusters by partition interaction between monolayers on the nanoparticle surface and the non-polar C8 HPLC sorbent, following a reverse-phase chromatography mechanism (Jimenez et al. 2003).

An ion-exchange mechanism involving gold clusters and the chromatographic column material were employed by Jahanshahi et al. (2005) and Bas et al. (1998) for nanoparticle purification with yields six times higher than ultrafiltration (Jahanshahi et al. 2005). Direct dependence of surface charge on size of the particle on charged nanoparticles enabled size separation of Au nanoparticles by capillary zone electrophoresis CZE (Schnabel et al. 1997) and carbon nanotubes by capillary gel electrophoresis and capillary electrochromatography (Xu et al. 2004).

Clearly, much remains to be done to extend both existing and new separations technologies to the growing collection of nanomaterials being produced in the research laboratory. These methods will prove critical to the commercialization of nanotechnologies, given the often radical differences in nature between the different sizes of like materials.

Deposition of nanomaterials

Several prototypes of continuous flow microreactors for the deposition of nanomaterials have been reported by our group (Chang et al. 2006; Mugdur et al. 2007; Hodes 2003; Liu and Chang 2007). For example, a microreactor was built to study the fundamental aspects of Chemical Bath Deposition (CBD) (Mugdur et al. 2007). CBD is an aqueous analogue of Chemical Vapor Deposition (CVD). The constituent ions are dissolved in an aqueous solution, and the thin films are produced through a heterogeneous surface reaction. It is known that CBD is capable of producing an epitaxial layer on a single crystal surface. Many compound semiconductors that are major candidates for solar energy utilization have been deposited by CBD, such as CdS, CdSe, Cu_2S, Cu_2Se, PbS, SnO, TiO_2, ZnO, ZnS, ZnSe, CdZnS, $CuInS_2$, and $CuInSe_2$ etc. (Hodes, 2003). CBD CdS is critical in fabricating high efficiency CdTe and $CuInSe_2$ thin film solar cells. The fundamental aspects of CBD are similar to that of a CVD process. It involves mass transport of reactants, adsorption, surface diffusion, reaction, desorption, nucleation, and growth. Fundamental understanding of CBD, however, is far less developed than CVD. This has limited the development and application of this growth technique. CBD is normally carried out as a batch process in a beaker and involves both heterogeneous and homogeneous reactions. Furthermore, the bath conditions change progressively as a function of time. It is necessary to find a method to decouple the homogeneous particle formation and deposition from the molecular level heterogeneous surface reaction.

A continuous flow microreactor was built to achieve this goal. The reactant streams were dispensed through two syringe pumps and allowed to mix in an interdigital micromixer. Fluids to be mixed are introduced into the mixing element as two counter-flows and enter interdigital channels (~20–50 μm) then split into many interpenetrated substreams. The substreams leave the interdigital channel perpendicular to the direction of the feed flows, initially within a multilayered structure. Fast mixing through diffusion follows due to the small thickness of the individual fluid layers. The resulting mixture from the micromixer then is passed through a temperature-controlled microchannel before it is impinged on a temperature-controlled substrate. The homogeneous chemistry of the impinging flux could be controlled precisely by the inlet concentrations, temperature, and most importantly the residence time.

Using this continuous flow microreactor, we have obtained particle free fluxes capable of depositing high quality CdS thin films. Smooth, dense, and highly oriented CdS thin films were deposited in shorter time with less chemical usage and waste. Figure 10 shows the AFM images of the CBD deposited CdS surfaces for (a) continuous flow microreactor and (b) batch process. These images demonstrate the capability of using the continuous flow microreactor to obtain a dense and uniform deposition. The XRD pattern given in Fig. 10c clearly demonstrates a highly (111) oriented cubic CdS thin film produced by the continuous flow microreactor at low temperature.

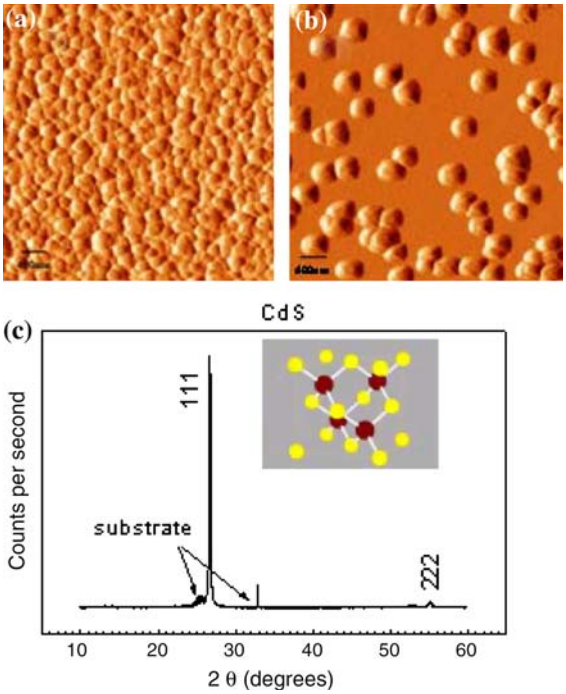

Fig. 10 Results from continuous flow microreactor for CBD (Chang et al. 2006; Mugdur et al. 2007)

A similar approach was also used to deposit nanostructured zinc oxide (Han et al. 2007) and ceria (Tseng and Paul 2007) thin films. This technique follows a thin film growth mechanism based on nanoparticle formation and deposition which was named Chemical Nanoparticle Deposition (CND) or Microreactor-Assisted Nanoparticle Deposition (MAND). ZnO thin films were deposited that is highly transparent and nanocrystalline exhibiting a larger bandgap, 4.35 eV compared to 3.4 eV of bulk ZnO, due to quantum size effects (see Fig. 11). Furthermore, we have fabricated uniform thin films of ceria polyhedral crystals and nanorods using room-temperature cerium nitrate precipitation chemistries (see Fig. 12) (Chang and Chen 2005). The microreactor produced a uniformly deposited thin layer of

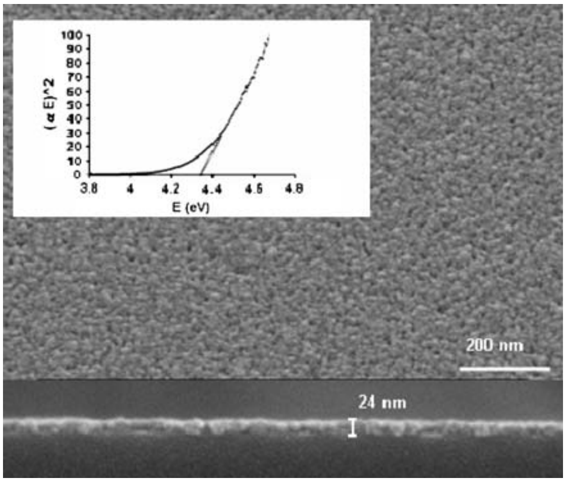

Fig. 11 Top and cross-sectional SEM images of ZnO thin film and estimated bandgap (inset) (Han et al. 2007)

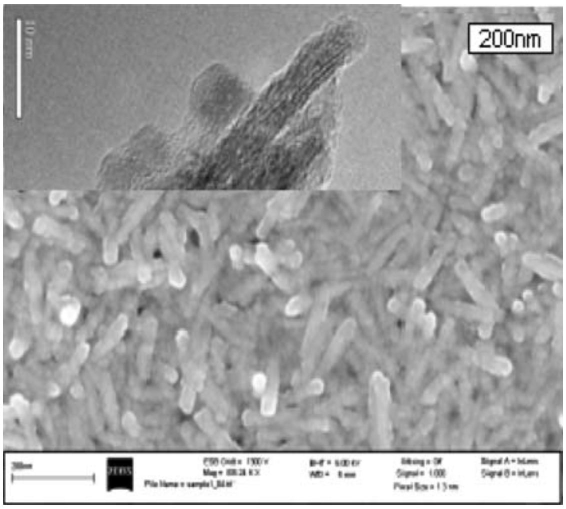

Fig. 12 SEM and HRTEM images of thin film CeO_2 nanorods (Tseng and Paul 2007)

nanorods in seconds. In contrast, batch processed films that have been made using the same chemistries produced large, uncontrolled aggregates. In addition, we were able to produce a variety of ZnO structures using our continuous flow microreactor by varying the concentration of NaOH, which was used for the precipitation. It was found that the concentration of NaOH exerted a great influence on the morphology of the synthesized ZnO. The flower-like ZnO structure was fabricated on the substrate at a higher NaOH concentration, while the chrysanthemum-like ZnO structure was grown at a lower one. These assembled ZnO structure have been deposited onto a substrate to form nanostructured thin films.

Polyamide dendrons and dendrimers have been synthesized using a continuous-flow microreactor. Furthermore, the synthesized polyamide dendrons were deposited onto functionalized glass surface through the formation of amide bond using a facile coupling procedure via a micromixer (Liu and Chang 2007). The dendron deposition process involved two major steps: the functionalization of the native glass surface using 3-aminopropyl triethoxysilane followed by coupling of the synthesized polyamide dendron with an aminosilanised surface. Compared with the conventional synthesis method, the microreactor provides a comparable yield, selectivity and a considerably faster synthesis rate. Nanostructured polyamide G1 dendron thin films could be deposited using an impinging flux from this microreactor in minutes.

Integration of bulk synthesis with nanoparticle processing

Theoretical and experimental approaches need to be developed for integrating the stages of nanoparticle synthesis and use. The theoretical aspects of integration involve linking process models related to shape forming with microchannel reactor and nanoparticle synthesis design criteria that generate specific particle attributes (size, shape, purity) and throughput. A potential area of integration of bulk synthesis to nanoparticle production involves directing the reaction product from the microchannels directly into a compaction press for fabricating small pellets for further sintering analysis. The concept for integrating the microchannel reactor to a compaction press using a sliding feed shoe is shown in Fig. 13. It allows for creating components from nanoparticles directly after synthesis. The feed shoe will have two inlets. The first inlet will be to the microreactor. The second inlet will be to a lubricant delivery system that tribostatically applies an organic lubricant on the inside of the die to reduce friction at the die-wall. The lubricant will also provide protection of the compacted nanoparticles prior to sintering. The press will be placed in an inert air/moisture-free chamber to avoid exposure to the ambient. Issues pertaining to flowability of the nanoparticles will have to be resolved using this

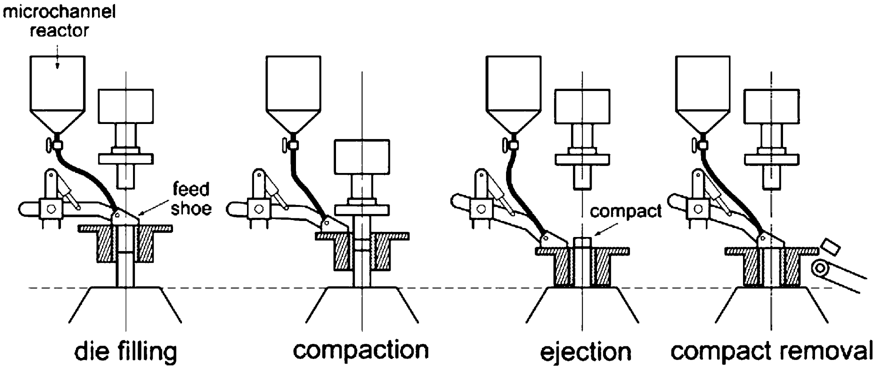

Fig. 13 An example of integrating bulk synthesis with nanoparticle consolidation

approach using a combination of fluidization, tribostatic and electrostatic principles. As another example of process integration, variations of this feed shoe technique could be developed to introduce the nanoparticles into a high intensity mixer. Here the nanoparticles could be combined with surfactant and binder additives in an inert atmosphere before being further processed by conventional powder processing techniques such as injection molding, extrusion, slip casting and tape casting. A third example is to direct the production of nanoparticles with polymer mixing into a molding operation similar to reaction injection molding or gas-pressure assisted molding that is currently prevalent in the world of plastics. The commercial implications from success in this program are enormous as they range from automotive and energy generation to petrochemical processing and aerospace.

Summary

Microreactor technology has the capacity to transform current batch nanoproduction practices into continuous processes with rapid, uniform mixing and precise temperature control. The advantages of microreaction technology have been shown by several research groups. It is expected that the field of nanoproduction can be advanced using the improved process control made available within highly-parallel, process-intensified microreactors. Clearly, much remains to be done to develop scale-up and post synthesis processes to take full advantage of this emerging field.

Acknowledgments Helpful input from Santosh Tiwari, Daniela Hutanu, Jack T. Rundel, Yu-Jen Chang and Shu-hong Liu is greatly appreciated. The authors would also like to acknowledge the financial support from the Air Force Research Laboratory FA8650-05-1-5041, the W.M. Keck Foundation 031879, the National Science Foundation CAREER CBET-0348723, and CBET-0654434.

References

Ajmera SK, Delattre C, Schmidt MA, Jensen KF (2002) Microfabricated differential reactor for heterogeneous gas phase catalyst testing. J Catal 209:401–412

Akthakul A, Hochbaum AI, Stellacci F, Mayes AM (2005) Size fractionation of metal nanoparticles by membrane filtration. Adv Mater 17(5):532–535

Al-Somali AM, Krueger KM, Falkner JC, Colvin VL (2004) Recycling size exclusion chromatography for the analysis and separation of nanocrystalline gold. Anal Chem 76:5903–5910

Amador C, Gavriilidis A, Angeli P (2004) Flow distribution in different microreactor scale-out geometries and the effect of manufacturing tolerances and channel blockage. Chem Eng J 101:379–390

Bas W, Steggerda JJ, Yan S, Casalnuovo JA, Mueting AM, Pignolet LH (1998) Separation of cationic metal cluster compounds by reversed-phase HPLC. Inorg Chem 27(5):948–951

Bejan A, Errera MR (1997) Deterministic tree networks for fluid flow: geometry for minimal flow resistance between a volume and one point. Fractals 5:685–695

Bouquey M, Serra C, Prat L, Hadziioannou G (2007) Microfluidic synthesis and assembly of reactive polymer beads to form new structured polymer materials. Book of abstracts, 9th international conference on microreaction technology, pp 104–105

Chan EM, Mathies RA, Alivisatos AP (2003) Size-controlled growth of CdSe nanocrystals in microfluidic reactors. Nano Lett 3(2):199–201

Chan EM, Alivisatos AP, Mathies RA (2005) High-temperature microfluidic synthesis of CdSe nanocrystals in nanoliter droplets. J Am Chem Soc 127:13854–13861

Chang HY, Chen HI (2005) Morphological evolution for CeO_2 nanoparticles synthesized by precipitation techniques. J Cryst Growth 283:457–468

Chang YJ, Mugdur PH, Han S-Y, Morrone AA, Ryu SO, Lee TJ, Chang C-H (2006) Nanocrystalline CdS MISFETs fabricated by a novel continuous flow microreactor. Electrochem Solid-State Lett 9(5):G174–G177

Chattopadhyay D, Lastella S, Kim S, Papadimitrakopoulos F (2002) Length separation of zwitterion-functionalized single wall carbon nanotubes by GPC. J Am Chem Soc 124:728–729

Commenge JM, Falk L, Corriou JP, Matlosz M (2002) Optimal design for flow uniformity in microchannel reactors. AIChE J 48(2):345–348

deMello AJ (2006) Control and detection of chemical reactions in microfluidic systems. Nature 442:394–402

deMello JC, deMello AJ (2004) Microsacle reactors: nanoscale products. Lab Chip 4:11N–15N

Edel JB, Fortt R, deMello JC, deMello AJ (2002) Microfluidic routes to the controlled production of nanoparticles. Chem Commun 10:1136–1137

Ehrfeld W, Hessel V, Lowe H (2000) Microreactors: new technology for modern chemistry. Wiley-VCH Verlag GmbH, Weinheim

Elimelech M, Gregory J, Jia X, Williams RA (1998) Particle deposition & aggregation, measurement, modeling and simulation. Butterworth-Heinemann

Fournier MC, Falk L, Villermaux J (1996) A new parallel competing reaction system for assessing micromixing efficiency—experimental approach. Chem Eng Sci 51(22):5053–5064

Gautam D, Benson HAE, Yan C (2005) Comparison of diafiltration and tangential flow filtration for purification of nanoparticle suspensions. Pharm Res 22(12):2152–2162

Glasgow I, Aubry N (2003) Enhancement of microfluidic mixing using time pulsing. Lab Chip 3:114–120

Han S-Y, Chang Y-J, Lee D-H, Ryu SO, Lee T-J, Chang C-H (2007) Chemical nanoparticle deposition of transparent ZnO thin films. Electrochem Solid-State Lett 10(1):K1–K5

Hessel V, Hardt S, Lowe H (2004) Chemical micro process engineering fundamentals, modeling and reactions. Wiley-VCH

Hodes G (2003) Chemical solution deposition of semiconductor films. Marcel Dekker, New York

Huang L, Wang D, Tang H, Wang S (2006) Separation and purification of nano-Al13 by UF method. Colloids Surf A Physicochem Eng Asp 275:200–208

Idelchik IE (1991) Fluid dynamics of industrial equipment: flow distribution design methods. Taylor & Francis, London

Idelchik IE (1994) Handbook of hydraulic resistance. CRC Press, Boca Raton

Ismagilov RF (2003) Integrated microfluidic systems. Angew Chem Int Ed 42:4130–4132

Jahanshahi M, Zhang Z, Lyddiatt A (2005) Subtractive chromatography for purification and recovery of nanobioproducts. IEE Proc Nanobiotechnol 152(3):121–126

Jimenez VL, Leopold MC, Mazzitelli C, Jorgenson JW, Murray RW (2003) HPLC of monolayer-protected gold nanoclusters. Anal Chem 75:199–206

Jongen N, Donnet M, Bowen P, Lemaître J, Hofmann H, Schenk R, Hofmann C, Aoun-Habbache M, Guillemet-Fritsch M, Sarrias J, Rousset A, Viviani M, Buscaglia MT, Buscaglia V, Nanni P, Testino A, Herguijuela JR (2003) Development of a continuous segmented flow tubular reactor and the "scale-out" concept—in search of perfect powders. Chem Eng Technol 26(3):303–305

Khan SA, Günther A, Schmidt MA, Jensen KF (2004) Microfluidic synthesis of colloidal silica. Langmuir 20:8604–8611

Kockmann N (2006) Transport processes and exchange equipment. In: Kockmann N (ed) Micro process engineering, chapter 3. Wiley-VCH

Krishnadasan S, Tovilla J, Vilar R, deMello AJ, deMello JC (2004) On-line analysis of CdSe nanoparticle formation in a continuous flow chip-based microreactor. J Mater Chem 14:2655–2660

Kroon J, Chang C-H, Nwachukwu F, Paul BK (2003) Investigations of microreaction technology for the production of semiconductor nanocrystals. In: 7th international conference on microreaction technology

Krueger KM, Al-Somali AM, Falkner JC, Colvin VL (2005) Characterization of nanocrystalline CdSe by size exclusion chromatography. Anal Chem 77:3511–3515

Lin XZ, Terepka AD, Yang H (2004) Synthesis of silver nanoparticles in a continuous flow tubular microreactor. Nano Lett 4(11):2227–2232

Liu S, Chang C-H (2007) High rate convergent synthesis and deposition of polyamide dendrimers using a continuous-flow microreactor. Chem Eng Technol 30(3):334–340

Liu S, Chang C-H, Paul BK, Remcho VT, Abhinkar B (2006) Synthesis of dendrimers using continuous flow microreactors. In: Proceedings of 2006 AIChE spring national meeting

Liu S, Chang C-H, Paul BK, Remcho VT (2008) Convergent synthesis of polyamido dendrimer using a continuous flow microreactor. Chem Eng J 135S:S333–S337

Mies MJM, Rebrov, DeCroon, MHJM, Schouten, JC, Ismagilov IZ (2006) Inlet section for micro-reactor. Patent PCT/NL2006/050074

Mugdur PH, Chang YJ, Han S-Y, Su Y-W, Morrone AA, Ryu SO, Lee T-J, Chang C-H (2007) A comparison of chemical bath deposition of CdS from a batch reactor and a continuous-flow microreactor. J Electrochem Soc 154(9):D482–D488

Munson BR, Young DF, Okiishi TH (1994) Fundamentals of fluid mechanics, 2nd edn. John Wiley and Sons, Inc., NY

Nagasawa H, Tsujiuchi T, Maki T, Mae K (2007) Controlling fine particle formation processes using a concentric microreactor. AIChE J 53(1):196–206

Nakamura H, Yamaguchi Y, Miyazaki M, Maeda H, Uehara M, Mulvaney P (2002) Preparation of CdSe nanocrystals in micro-flow-reactor. Chem Commun 23:2844–2845

Niyogi S, Hu H, Hamon MA, Bhowmik P, Zhao B, Rozenzhak SM, Chen J, Itkis ME, Meier MS, Haddon RC (2001) Chromatographic purification of soluble single-walled carbon nanotubes (s-SWNTs). J Am Chem Soc 123:733–734

Paul BK (2005) Micro energy and chemical systems and multiscale fabrication. In: Micromanufacturing and nanotechnology, chapter 14. Springer-Verlag, Germany

Paul BK, Peterson RB (1999) Microlamination for microtechnology-based energy, chemical, and biological systems. In: ASME IMECE, vol. 39. Nashville, Tennessee, AES, November 15–20, pp 45–52

Rebrov EV, Duinkerke SA, Schouten JC (2003) Optimization of heat transfer characteristics, flow distribution, and reaction processing for a microstructured reactor/heat-exchanger for optimal performance in platinum catalyzed ammonia oxidation. Chem Eng J 93:201–216

Rebrov EV, Ismagilov IZ, Ekatpure RP, DeCroon MHJM, Schouten JC (2007) Header design for flow equalization in microstructured reactors. AIChE J 53(1):28–38

Riman IS, Cherepkova VG (1973) An approximate method for calculation of flow field in a tube filled with tick-walled bars. Ind Aerodyn 30:65–74

Ritter M (2002) Nanostructured materials. Ceram Bull 81(3):33–36

Rundel JT, Paul BK, Remcho VT (2007) Organic solvent nanofiltration for microfluidic purification of poly(amidoamine) dendrimers. J Chromatogr A 1162(2, 31):
167–174

Schenk R, Hessel V, Hofmann C, Kiss J, Löwe H, Ziogas A (2004) Numbering-up of micro devices: a first liquid-flow splitting unit. Chem Eng J 101:421–429

Schenk R, Hessel V, Hofmann C, Löwe H, Schonfeld F (2003) Novel liquid-flow splitting unit specifically made for numbering-up of liquid-liquid chemical microprocessing. Chem Eng Technol 26(12):1271–1280

Schnabel U, Fischer Ch-H, Kenndler E (1997) Characterization of colloidal gold nanoparticles according to size by capillary zone electrophoresis. J Microcolumn Sep 9(7): 529–534

Shestopalov I, Tice JD, Ismagilov RF (2004) Multi-step synthesis of nanoparticles performed on millisecond time scale in a microfluidic droplet-based system. Lab Chip 4:316–321

Siebrands T, Giersig M, Mulvaney P, Fischer Ch-H (1993) Steric exclusion chromatography of nanometer-sized gold particles. Langmuir 9:2297–2300

Sounart TL, Safier PA, Voigt JA, Hoyt J, Tallant DR, Matzke CM, Michalske TA (2007) Spatially-resolved analysis of nanoparticle nucleation and growth in a microfluidic reactor. Lab Chip 7:908–915

Sovran G, Klomp ED (1967) Experimentally determined optimum geometries for rectilinear diffusers with rectangular, conical or annular cross-section. Fluid mechanics of internal flow. Elsevier, Amsterdam

Sweeney SF, Woehrle GH, Hutchison JE (2006) Rapid purification and size separation of gold nanoparticles via diafiltration. J Am Chem Soc 128:3190–3197

Takagi M, Maki T, Miyahara M, Mae K (2004) Production of titania nanoparticles by using a new microreactor assembled with same axle dual pipe. Chem Eng J 101:269–276

Taylor RA, Penney WR, Vo HX (2005) Scale-up methods for fast competitive chemical reactions in pipeline mixers. Ind Eng Chem Res 44:6095–6102

Tishchenko G, Luetzow K, Schauer J, Albrecht W, Bleha M (2001) Purification of polymer nanoparticles by diafiltration with polysulfone/hydrophilic polymer blend membranes. Sep Purif Technol 22–23:403–415

Trachsel F, Günther A, Khan S, Jensen KF (2005) Measurement of residence time distribution in microfluidic systems. Chem Eng Sci 60:5729–5737

Tseng CT, Paul BK (2007) Comparison of batch mixing and micromixing approaches in the synthesis and deposition of ceria nanoparticles. Transactions of NAMRI, 35

Wagner J, Köhler JM (2005) Continuous synthesis of gold nanoparticle in a microreactor. Nano Lett 5(4):685–691

Wang H, Nakamura H, Uehara M, Miyazaki M, Maeda H (2002) Preparation of titania particles utilizing the insoluble phase interface in a microchannel reactor. Chem Commun 14:1462–1463

Wei G-T, Liu F-K (1999) Separation of nanometer gold particles by size exclusion chromatography. J Chromatogr A 836:253–260

Wei G-T, Liu F-K, Wang CRC (1999) Shape separation of nanometer gold particles by size-exclusion chromatography. Anal Chem 71:2085–2091

Wiessmeier G, Honicke D (1998) Strategy for the development of microchannel reactors for heterogeneously catalyzed reactions. In: Proceedings of the second international conference on microreaction technology, vol 24. AIChE, New Orleans, pp 24–32

Wilcoxon JP, Martin JE, Provencio P (2000) Size distributions of gold nanoclusters studied by liquid chromatography. Langmuir 16:9912–9920

Xu X, Ray R, Gu Y, Ploehn HJ, Gearheart L, Raker K, Scrivens WA (2004) Electrophoretic analysis and purification of fluorescent single-walled carbon nanotube fragments. J Am Chem Soc 126:12736–12737

Yen BKH, Scott NE, Jensen KF, Bawendi MG (2003) A continuous-flow microcapillary reactor for the preparation of a size series of CdSe nanocrystals. Adv Mater 15(21):1858–1862

Yen BKH, Gunther A, Schmidt MA, Jensen KF, Bawendi MG (2005) A microfabricated gas–liquid segmented flow reactor for high-temperature synthesis: the case of CdSe quantum dots. Angew Chem Int Ed 44:5447–5451

Zhao B, Hu H, Niyogi S, Itkis ME, Hamon MA, Bhowmik P, Meier MS, Haddon RC (2001) Chromatographic purification and properties of soluble single-walled, carbon nanotubes. J Am Chem Soc 123:11673–11677